Birkbeck ePrints: an open access repository of the research output of Birkbeck College

http://eprints.bbk.ac.uk

Harvey,K.; Duguid I.C.; Alldred, M.J.; Beatty, S.E.; Ward H.; Keep N.H. et al (2004). The GDP-GTP exchange factor collybistin: an essential determinant of neuronal gephyrin clustering. *The Journal of Neuroscience* 24 (25) 5816-5826.

THE GDP-GTP EXCHANGE FACTOR COLLYBISTIN: AN ESSENTIAL DETERMINANT OF NEURONAL GEPHYRIN CLUSTERING

Kirsten Harvey[1], Ian C. Duguid[2†], Melissa J. Alldred[3†], Sarah E. Beatty[4], Hamish Ward[4], Nicholas H. Keep[5], Sue E. Lingenfelter[3], Brian R. Pearce[1], Johan Lundgren[6], Michael J. Owen[7], Trevor G. Smart[2], Bernhard Lüscher[3], Mark I. Rees[4,8] and Robert J. Harvey[1]*

[1]Dept. of Pharmacology, The School of Pharmacy, 29-39 Brunswick Square, London WC1N 1AX, UK; [2]Dept. of Pharmacology, University College London, Gower Street, London WC1E 6BT, UK; [3]Dept. of Biology and Dept. of Biochemistry and Molecular Biology, Penn State University, University Park, PA 16802, USA; [4]Dept. of Molecular Medicine, Faculty of Medical and Health Sciences, University of Auckland, Private bag 92019, Auckland, New Zealand, [5]School of Crystallography, Birkbeck, University of London, Malet Street, London WC1E 7HX and [6]Dept. of Pediatrics, University Hospital, SE-221 85 Lund, Sweden, [7]Psychological Medicine, University of Wales College of Medicine, Cardiff CF14 4XN, UK, and [8]Swansea Clinical School, Grove Building, University of Wales, Swansea SA2 8PP, UK

*Correspondence and proofs to: Robert J. Harvey, Department of Pharmacology
The School of Pharmacy, 29-39 Brunswick Square
London WC1N 1AX, United Kingdom
Telephone: (44) 207 753 5930
FAX: (44) 207 753 5902
E-mail: robert.harvey@ulsop.ac.uk

†These authors contributed equally to this study.

Running title: Collybistin and gephyrin clustering

Manuscript Information: Pages: **32**; Figures: **7**; Tables: **0**; Equations: **0**

Word count: Abstract: **236** words; Introduction: **511** words; Discussion: **1449** words.

Keywords: epilepsy; GABA$_A$ receptor; glycine receptor; hyperekplexia; trafficking

Abstract

Glycine receptors and specific subtypes of GABA$_A$ receptors are clustered at synapses by the multi-domain protein gephyrin, which is in turn translocated to the cell membrane by the GDP-GTP exchange factor (GEF) collybistin. We report the characterization of several new variants of collybistin, which are created by alternative splicing of exons encoding an N-terminal *src* homology 3 (SH3) domain and three alternate C-termini (CB1, CB2 and CB3). The presence of the SH3 domain *negatively* regulates the ability of collybistin to translocate gephyrin to submembrane microaggregates in transfected mammalian cells. Since the majority of native collybistin isoforms appear to harbor the SH3 domain, this suggests that collybistin activity may be regulated by protein-protein interactions at the SH3 domain. We have localized the binding sites for collybistin and the GlyR β subunit to the C-terminal MoeA homology domain of gephyrin and show that multimerization of this domain is required for collybistin-gephyrin and GlyR-gephyrin interactions. We further demonstrate that gephyrin clustering in recombinant systems and cultured neurons requires both collybistin-gephyrin interactions and an intact collybistin pleckstrin homology domain. The vital importance of collybistin for inhibitory synaptogenesis is underlined by the discovery of a mutation (G55A) in exon 2 of the human collybistin gene (*ARHGEF9*) in a patient with clinical symptoms of both hyperekplexia and epilepsy. The clinical manifestation of this collybistin missense mutation may result, at least in part, from mislocalization of gephyrin and a major GABA$_A$ receptor subtype.

Inhibitory neurotransmission relies on glycine and γ-aminobutyric acid (GABA) receptors being clustered at postsynaptic specializations opposite axon terminals releasing the corresponding neurotransmitters. Central to this arrangement is gephyrin, which co-localizes with GlyRs at inhibitory synapses (Triller et al., 1985; Schmitt et al., 1987). Gephyrin can interact with polymerized tubulin (Kirsch et al., 1991), the GlyR β subunit (Kneussel et al., 1999a), profilin (Mammoto et al., 1998), RAFT-1 (Sabatini et al., 1999), dynein light chains 1 and 2 (Fuhrmann et al., 2002) and Mena/VASP (Giesemann et al., 2003). In addition, gephyrin is also essential for the postsynaptic clustering of GABA$_A$ receptors containing α2 or α3 subunits (Essrich et al., 1998; Kneussel et al., 1999b, 2001b; Levi et al., 2004). A selective loss of synaptic GABA$_A$ receptors in γ2 subunit mutant mice also results in the loss of gephyrin clusters (Essrich et al., 1998; Schweizer et al., 2003), indicating some interdependence for their synaptic localisation. Interestingly, when expressed in mammalian cells, gephyrin forms cytoplasmic aggregates (Kirsch et al., 1995), suggesting that other 'factors' are required to direct gephyrin to submembrane microaggregates. The preliminary characterization of collybistin (Kins et al., 2000; Grosskreutz et al., 2001), a novel gephyrin-associated GDP-GTP exchange factor (GEF), presented a plausible mechanism(s) by which gephyrin could be targeted to synapses.

Collybistin is a member of the guanine nucleotide exchange factor (GEF) superfamily, which catalyze GTP-GDP exchange on small GTPases of the Rho family (Wherlock and Mellor, 2002). GEFs are characterized by tandem exchange factor (RhoGEF) and pleckstrin homology (PH) domains. The RhoGEF domain catalyses the exchange reaction, while the PH domain can bind with high affinity to membrane phosphoinositides, thus restricting GEF localization and activity to the submembrane compartment (Kavran et al., 1998). Collybistin was initially found in two isoforms created by alternative splicing: 'collybistin I', which contains an N-terminal src homology 3 (SH3) domain and a C-terminal coiled-coil domain, and 'collybistin II', which lacks the SH3 domain and has an alternate C-terminus. On expression in HEK293 cells, collybistin I co-localized with intracellular gephyrin aggregates, whilst collybistin II enabled translocation of

2

gephyrin to submembrane microaggregates (Kins et al., 2000). The human homologue of collybistin, hPEM-2 (human homologue of Posterior End Mark-2) appears to activate the GTPase Cdc42 (Reid et al., 1999), which influences cell morphology by initiating actin cytoskeleton remodeling (Erickson and Cerione, 2001). It has been proposed that at inhibitory synapses, collybistin initiates local re-modeling of the subsynaptic cytoskeleton (Kneussel and Betz, 2000).

In this study, we investigated the diversity of collybistin isoforms generated by alternative splicing and the role of the SH3, RhoGEF and PH domains in translocating gephyrin to submembrane microaggregates. We also mapped the binding sites for collybistin and the GlyR β subunit on gephyrin. This information was used to evaluate *ARHGEF9* as a candidate gene for hyperekplexia in a cohort of thirty-two patients without mutations in the GlyR α1 and β subunit genes or gephyrin (Rees et al., 2001, 2002, 2003). Examination of naturally-occurring and artificial mutants of collybistin emphasizes the importance of this RhoGEF for postsynaptic localization of gephyrin and inhibitory ligand-gated ion channels.

Materials and Methods

Amplification, cloning and sequencing of rat and human collybistin cDNAs

Rat collybistin cDNAs were amplified from postnatal (P0) rat spinal cord and whole-brain first-strand cDNA using the primer combinations r1: 5'-GTGGGGATCCATGCAGTGGATTAGAGGCGGA-3' plus r2: 5'-TTCGAATTCCCCATCCTCCTGGTTCACCCA-3' and r3 5'-GGAGGATCCAATACGTTGGCTTAGAGCTTT-3' plus r4 5'-TTAGAATTCTCTGCCTTCCTATAGGTATTA-3'. Human collybistin cDNAs were amplified from human whole-brain or spinal cord cDNA (Clontech) using the primer combinations h1: 5'-CATGGCCTCGCTGTGATATGTATG-3' plus h2: 5'-TCCAGGTGTCCGTTCTGCACATCG-3' or h3 5'-CTGCAATGACTGTGAGAAAAGTCC-3' plus h4 5'-ATTATCTGCCTCCCTGTAGGTATC-3'. Amplifications were performed under semi-quantitative conditions using *Pfu* Turbo proofreading DNA polymerase (Stratagene) and 30 cycles of 94ºC for 1 min, 65ºC for 1 min and 68ºC for 3 min. PCR products were cloned into the

pCR4 Blunt TOPO vector (Invitrogen), and plasmid DNAs were made using spin miniprep and maxi kits (QIAGEN). Plasmid inserts were fully sequenced using the BigDye ready reaction mix (Perkin-Elmer/Applied Biosystems) and an Applied Biosystems 310 automated DNA sequencer.

Functional assays of collybistin/gephyrin interactions in HEK293 cells

pRK5myc-CB2$_{SH3+}$, *pRK5myc-CB2$_{SH3-}$* and *pRK5myc-CB3$_{SH3+}$*: collybistin cDNAs were amplified from postnatal (P0) rat brain first-strand cDNA using the primers r1 and r4 (see above) and cloned into the *Bam*HI and *Eco*RI sites of the vector pRK5myc so that a 9E10 (myc) tag is attached to the N-terminus. Deletions of the SH3, RhoGEF and PH domains were made in *pRK5myc-CB2$_{SH3-}$* using the Quikchange site directed mutagenesis kit (Stratagene). *pEGFP-gephyrin*: the entire coding region of the rat gephyrin P1 isoform (Prior et al., 1992) was amplified from postnatal (P0) rat brain first-strand cDNA using the primers rGeph1 5'-CGCTGATCAACATGGCGACCGAGGGA-3' and rGeph2 5'-TGGCTCGAGTCATAGCCGTC CGATGA-3', cut with *Bcl*I and *Xho*I, and cloned into the *Bgl*II and *Sal*I sites of pEGFP-C2 (Clontech), so that the EGFP tag is N-terminal. *pDsRed-GlyR β*: the large intracellular loop of the human GlyR β subunit (Handford et al., 1996) was amplified using the primers hβDsRed1 5'-GCTGAATTCGCCACCATGGCAGTTGTCCAGGTGATGCT-3' and hβDsRed2 5'-AACGGAT CCCTTGCATAAAGATCAATTCGC-3' and cloned into the *Eco*RI and *Bam*HI sites of pDSRedN1 (Clontech), so that the DsRed tag is C-terminal. Amplifications were performed using *Pfu* Turbo DNA polymerase and all plasmids were sequenced to confirm the veracity of the constructs. HEK293 cells (ATCC CRL1573) were grown in Dulbecco's modified Eagle's medium (DMEM) supplemented with 10% (v/v) fetal bovine serum, 2 mM glutamine, 100U/ml penicillin G and 100 µg/ml streptomycin at 37°C in 95% air-5% CO_2 (Harvey et al., 1999). Exponentially growing cells were electroporated (400V, infinite resistance, 125 µF; BioRad Gene Electropulser II) with various combinations of the plasmid constructs. For co-transfections (e.g. myc-CB2$_{SH3-}$ plus EGFP-gephyrin) plasmids were used at a ratio of 1:1. After 24 h, cells were washed twice in PBS and fixed for 5 min in 4% (w/v) PFA in PBS. Myc-tagged CB2$_{SH3+}$, CB2$_{SH3-}$ and CB3$_{SH3+}$

proteins were detected using an anti-9E10 monoclonal antibody (Sigma) and TRITC- or Cy5-conjugated secondary antibodies (Jackson ImmunoResearch, Westgrove, PA) using standard protocols. Confocal microscopy was performed as previously described (Dunne et al., 2002).

Culture, transfection and immunostaining of cortical neurons

Cortical neurons were cultured from embryonic day (E) 14 mice. Cortical hemispheres were collected in phosphate buffered saline (PBS, pH 7.4) containing 5.5 mM glucose and treated with papain (0.5 mg/ml, Sigma, St. Louis, MO) and DNase I (10 μg/ml) in PBS containing 1 mg/ml bovine serum albumin and 10 mM glucose for 15 min at room temperature. The cells were mechanically triturated and then plated on poly-L-lysine coated glass coverslips at 4×10^4 cells/cm^2 in modified Eagle medium (MEM, Invitrogen, Carlsbad, CA) containing 10% v/v fetal bovine serum (FBS) which was replaced after 60 min. After 24 h the cover slips were turned upside down onto a glial feeder layer in a Petri dish containing Neurobasal-A supplemented with B27 (Invitrogen). Neurons were transfected at 18 days *in vitro* (DIV) using a calcium co-precipitation transfection kit (BD Biosciences, Palo Alto, CA). Briefly, the cover slips were re-inverted and transferred into new Petri dishes containing glia-conditioned Neurobasal A/B27 supplemented with 0.8 mg/ml $NaHCO_3$, 1 μM 6-cyano-7-nitoquinoxaline-2,3-dione (CNQX, Sigma, St. Louis, MO) and 100 μM 2-amino-5-phosphonovaleric acid (APV, Sigma, St. Louis, MO). Plasmid DNA (10 μg/cover slip) was mixed with 12.4 μl 2M $CaCl_2$ to a final volume of 100 μl and then added slowly to an equal volume of 2x Hepes-buffered saline while thoroughly mixing. The DNA was allowed to precipitate for 15 min, added to the cells and incubated for 45 min. The cover slips were then returned to the original dishes containing conditioned medium and used for immunocytochemistry at 21 DIV.

Neurons on coverslips were rinsed with PBS, fixed with 4% w/v PFA in 150 mM sodium phosphate buffer (pH 7.4) for 15 min, permeabilized for 5 min with 0.15% saponin in PBS containing 10% v/v normal donkey serum, and incubated overnight at 4ºC with combinations of

primary antibody to the myc tag of collybistin constructs (rabbit polyclonal Anti-Myc Tag, (Medical and Biological Laboratories CO., Nahgoya, JP), gephyrin (mAb7a, Alexis, San Diego, CA) or glutamic acid decarboxylase (mAb GAD-6, Developmental Studies Hybridoma Bank, University of Iowa) and the GABA$_A$ receptor γ2 subunit (raised in guinea pigs, Fritschy and Mohler, 1995) in PBS containing 0.15% v/v saponin and 10% v/v normal donkey serum. Note that for experiments with EGFP-gephyrin constructs, mAb7a is assumed to recognize both native <u>and</u> recombinant gephyrin. The cells were washed in PBS containing 0.15% v/v saponin and then incubated with secondary antibody raised in the proper species and conjugated to AlexaFluoro488 (Molecular Probes, Eugene, OR), Cy3 or Cy5 (Jackson ImmunoResearch Laboratories, Westgrove, PA), in PBS containing 0.15% v/v saponin and 10% v/v normal donkey serum. Epifluorescent images were captured using a Zeiss Axiophot2 microscope equipped with a 1.3 DIC 40x objective and a ORCA-100 cooled CCD camera linked to an Openlab imaging system (Improvision, Lexington, MA).

Quantitation of immunofluorescence images

To quantify the effects of transfecting wild-type or mutant collybistin and gephyrin constructs into neurons, two dendritic segments of 40 μm length were selected per cell (for 10-12 transfected cells per construct) that exhibited low overall background staining for gephyrin (mAb7a) or the GABA$_A$ receptor γ2 subunit. Immunoreactive puncta (size range 0.2 μm to 2 μm in diameter) in each segment were automatically selected by setting a fluorescence intensity threshold that was two-fold greater than the diffuse fluorescence on dendritic shafts within the region of interest. The average number of gephyrin (mAb7a) clusters was determined by counting the number of immunoreactive puncta within the correct size range per 40 μm segment per cell. The number of GABA$_A$ receptor clusters (punctate γ2 immunoreactivity) was determined identically on dendritic segments that were innervated by GABAergic terminals (as

6

judged by GAD staining). Analysis was performed using Openlab imaging software with Microsoft Excel. Student's two-tailed t-test was used for all statistical comparisons.

Mapping binding sites on gephyrin using the GAL4 yeast two-hybrid system

To identify putative domains of gephyrin which interact with the collybistin and the GlyR β subunit, several baits were cloned into the GAL4 binding domain vector pYTH9, which can be integrated into the *trp* locus for stable expression of fusion proteins (Fuller et al., 1998). *pYTH9-CB2_{SH3-}*: pRK5myc-CB2_{SH3-} was cut with *Nco*I and *Eco*RI to release the full-length cDNA, and this was cloned into the corresponding sites in pYTH9. *pYTH9-GlyR β*: the large intracellular loop of the human GlyR β subunit (Handford et al., 1996) was amplified using the primers hGlyRβ1 5'-GGT<u>GTCGAC</u>GAACAACCCCAAAAGGGTTGA-3' and hGlyRβ2 5'-AGG<u>GAAT TC</u>TCATCTTGCATAAAGATCAAT-3' and cloned into the *Sal*I and *Eco*RI sites of pYTH9. *pYTH9-MoeA*: the 'MoeA homology domain' from the rat gephyrin P1 isoform (Prior et al., 1992) was amplified using the primers rGeph3 5'-AGC<u>GTCGAC</u>CAGTGCTGTAGATATCA-3' and rGeph4 5'-TGG<u>CCGCGG</u>TCATAGCCGTCCGATGACCA-3' and cloned into the *Sal*I and *Sac*II sites of pYTH9. Fragments of the rat gephyrin P1 isoform cDNA were amplified using multiple oligonucleotide primers and were cloned into the vector pACT2 (Clontech). As above, amplifications were performed using *Pfu* Turbo DNA polymerase and all constructs were fully sequenced. Co-transformed yeast were plated on selective dropout media lacking leucine and tryptophan (Clontech) and incubated at 30°C for 3-6 days to allow prototropic colonies to emerge. *LacZ* reporter gene assays were performed as previously described (Fuller et al., 1998).

Collybistin gene structures and analysis in hyperekplexia patients

Human collybistin cDNAs (Reid et al., 1999 and this study) were submitted for <u>B</u>LAST-<u>L</u>ike <u>A</u>lignment <u>T</u>ool (BLAT) searches of the UCSC Genome Browser Database (Karolchik et al., 2003; http://genome.ucsc.edu/). Intron/exon organizations were established from comparisons of

cloned cDNAs, spliced ESTs and genomic sequences. The majority of patients included in the mutation analysis of the human collybistin gene (*ARHGEF9*) are described elsewhere (Rees et al., 2001). A further seven unrelated hyperekplexia patients were also analysed; all conform to the diagnostic criteria of inclusion which involves a history of neonatal hypertonia, a nose tap response and an exaggerated startle response leading to injurious fall down consequences with preservation of consciousness (Andrews and Owen, 1997). Exons and flanking intronic sequences, plus 5' and 3' untranslated regions were amplified from patient DNAs using the primers detailed in Table S1 (Rees et al., 2001, 2002). Each 25 µl reaction contained 60 ng of genomic DNA, 10 pmol of each primer, 1.5 mM $MgCl_2$, 50 mM KCl, 10 mM Tris-HCl pH 8.3, 200 µM of dNTPs (Pharmacia) and 1 U *Taq* polymerase (Qiagen). PCR conditions consisted of an initial denaturation at 94°C for 5 min followed by 35 cycles of 30 s at 94°C, 30 s at 60°C, 30 s at 72°C. Mutation analysis of PCR products was carried out using Transgenomics dHPLC HT-WAVE[R] DNA Fragment Analysis System, using DNASep[R] columns (Transgenomics). The program dHPLCMelt was used to predict the optimal melting conditions for PCR fragments and the WAVE instrument was run under partially denaturing conditions for mutation detection and SNP discovery. Due to the X-linked localization of *ARHGEF9*, all male patient PCRs were combined with a sequence-verified female DNA control. Variant dHPLC profiles suggestive of allelic heterogeneity were gel isolated (QIAGEN) and sequenced using ABI3100 technology. The G55A mutant was introduced into *pRK5myc-CB3$_{SH3+}$* using the Quikchange site directed mutagenesis kit (Stratagene).

Results

Multiple collybistin isoforms are generated by alternative splicing

Yeast two-hybrid screening with gephyrin originally identified two collybistin isoforms which were created by alternative splicing of primary transcripts (Kins et al., 2000). Alternative splicing of collybistin mRNAs appears to have functional relevance, since only collybistin II is able to translocate gephyrin to submembranous microaggregates (Kins et al., 2000). We carried out RT-

PCR assays from rodent/human spinal cord and whole-brain cDNAs to assess the relative abundance of different collybistin transcripts. DNA sequence analysis of both amplified and published cDNAs (Kins et al., 2000) revealed that *three* different collybistin C-termini can be specified in the rat by the use of different cassette exons (Fig. 1*A-D*). Collybistin I (GRVGEEENQSLELKRACEVLQRLWSPGKKS*) and collybistin II (VTQRKWHY*) C-termini are generated by insertion of either 109 bp or 62 bp exons into collybistin transcripts (Fig. 1*A,C*). When neither exon is utilized, a third C-terminus is specified which shares 59/60 residues with the C-terminus of human collybistin (hPEM-2; Reid et al., 1999). In contrast, the exon encoding the N-terminal SH3 domain is utilized in the majority of rodent and human collybistin brain mRNAs (Fig. 1*B*). Splicing of this exon did not alter during postnatal development in mouse brain (Fig. 1*B*).

Accordingly, we have renamed these collybistin isoforms CB1 (collybistin I), CB2 (collybistin II) and CB3 (hPEM2-like), and also denoted SH3 domain usage (e.g. $CB2_{SH3+}$ or $CB2_{SH3-}$). In postnatal rodent spinal cord and brain, our RT-PCR assays predict that the $CB2_{SH3+}$ and $CB3_{SH3+}$ isoforms are predominant (Fig. 1*B,C*). CB1 isoforms were not detected in any of our rodent mRNAs, but might be expressed in different tissues or at other developmental stages. To confirm these results, we cloned and sequenced full-length cDNAs for rat collybistin from rat whole-brain mRNA. Only $CB2_{SH3+}$ and $CB3_{SH3+}$ cDNAs were found, in a ratio of 5:4 (nine independent isolates). In human brain and spinal cord, only the $CB3_{SH3+}$ isoform was present; transcripts encoding CB1 and CB2 variants were not detected (Fig. 1*C*). Lastly, BLAST analysis revealed that rat collybistins and hPEM-2 are most closely related to ARHGEF4 (ASEF/KIAA1112; Kawasaki et al., 2000), Tiam-1 (Habets et al., 1994; Worthylake et al., 2000) and βPIX/p85Cool-1 (Bagrodia et al., 1998; Manser et al., 1998), all of which specifically activate the GTPase Rac1 but not Cdc42.

Functional domains of collybistin required for gephyrin submembrane targeting

Full-length cDNAs for $CB2_{SH3+}$ and $CB3_{SH3+}$ (Fig. S2) were tagged with the 9E10 epitope at the N-terminus of the expressed protein. To test the activity of these recombinant collybistin isoforms, we also created a plasmid construct (pEGFP-gephyrin) in which enhanced green fluorescent protein (EGFP) is fused to the N-terminus of gephyrin (P1 isoform, Prior et al., 1992). This allows discrimination of living cells possessing extensive submembrane microaggregates from those showing intracellular gephyrin deposits (Kins et al., 2000) using fluorescence microscopy. When transfected into HEK293 cells, myc-$CB2_{SH3-}$ is diffusely distributed throughout the cytoplasm (Fig. 1*E*). Although they were not serum-starved, some cells showing high levels of myc staining exhibited filopodia (MacKay and Hall 1998), while others also displayed membrane ruffling (Fig. 1*E*). In contrast, EGFP-gephyrin expression resulted in the formation of large intracellular deposits (Fig. 1*F*), which are consistent with those observed using non-tagged gephyrin (Kirsch et al., 1995). Co-expression of CB2 isoforms with EGFP-gephyrin revealed that the common SH3-containing variant (myc-$CB2_{SH3+}$) behaved exactly like collybistin I (Kins et al., 2000) and redistributed to large intracytoplasmic EGFP-gephyrin aggregates (Fig. 1*G*). In contrast, the variant lacking the SH3 domain (myc-$CB2_{SH3-}$), redistributed with EGFP-gephyrin to submembrane microaggregates in ~40% of co-transfected cells (Fig. 1*H,I*), while others demonstrated different phenotypes (e.g. intracellular aggregates with extended filamentous structures; data not shown). Transfection of HEK293 cells with myc-$CB2_{SH3-}$, EGFP-gephyrin and red fluorescent protein-conjugated GlyR β subunit intracellular loop (DSRed-GlyR β) resulted in collybistin-mediated translocation of EGFP-gephyrin to submembrane clusters, that were also decorated by DSRed-GlyR β (Fig. 2*A-D*). However, it is noteworthy that the expression of myc-$CB2_{SH3-}$ was not restricted to EGFP-gephyrin/DSRed-GlyR β clusters (Fig. 2*C,D*).

Functional analyses of collybistin isoforms and mutants in transfected neurons

To assess the possible contribution of collybistin to endogenous gephyrin clustering, we transfected selected collybistin constructs into cultured cortical neurons. Whereas collybistin has been speculated to represent a synaptic protein (Kins et al., 2000; Kneussel and Betz 2000), we found myc-CB2$_{SH3+}$ and myc-CB2$_{SH3-}$ to be diffusely distributed throughout the soma and dendrites of transfected cortical neurons (Fig. 3*A-D*). Recombinant myc-CB2$_{SH3+}$ and myc-CB2$_{SH3-}$ did not significantly affect endogenous gephyrin clustering (Fig. 3*E*). For myc-CB2$_{SH3+}$ the average number of gephyrin clusters was 9.96 ± 2.13 per 40 μm segment per cell versus 9.86 ± 2.27 for myc-CB2$_{SH3-}$ (n = 11 neurons per construct). The average cluster size was 1.60 ± 0.84 μm for myc-CB2$_{SH3+}$ versus 1.39 ± 0.47 for myc-CB2$_{SH3-}$ (n = 11 neurons per construct). We next attempted to construct dominant-negative mutants of CB2 (Fig. 3, inset), to test the proposed function of collybistin in gephyrin clustering in neurons. Deletions of the RhoGEF domain (amino acids 114-293) or the PH domain (amino acids 326-432) were made in the CB2$_{SH3-}$ isoform. On expression in HEK293 cells, deletion of the RhoGEF domain (myc-CB2$_{SH3-}$ΔRhoGEF) abolished gephyrin-collybistin co-localization and EGFP-gephyrin submembrane targeting (Fig. 3*F,G*). By contrast, deletion of the PH domain in myc-CB2$_{SH3-}$ (i.e. myc-CB2$_{SH3-}$ΔPH) resulted in the production of cytoplasmic collybistin-gephyrin aggregates (Fig. 3*H,I*), indicating that the PH domain was required for normal targeting of this protein. As expected, myc-CB2$_{SH3-}$ΔPH also interfered effectively with clustering of gephyrin in neurons: dendritic clusters of endogenous gephyrin (as visualized by immunostaining with mAb7a) were almost completely eliminated following expression of this deletion mutant (Fig. 3*J,K*). The average number of gephyrin clusters for myc-CB2$_{SH3-}$ΔPH was significantly reduced to 2.1 ± 1.13 clusters per 40 μm segment per cell (n = 10 neurons; Fig. 3*E*), when compared to either myc-CB2$_{SH3+}$ or myc-CB2$_{SH3-}$ (p<0.001, Student's t-test). Thus, myc-CB2$_{SH3-}$ΔPH effectively competes with endogenous collybistin for binding to gephyrin, causing mis-localization of endogenous gephyrin (arrowheads in Fig. 3*J,K*). Note that dendrites of non-transfected control cells demonstrated robust gephyrin clustering (Fig. 3*J*).

Mapping of binding sites for collybistin and the GlyR β subunit on gephyrin

Whereas the binding sites for gephyrin on collybistin and the GlyR β subunit have previously been described (Kneussel et al., 1999a; Grosskreutz et al., 2001), the corresponding binding sites on gephyrin have remained elusive. Several studies have suggested that the binding site for the GlyR β subunit lies within the N-terminal MogA domain (Meier et al., 2000; Xiang et al., 2001; Schwarz et al., 2001) or the 'linker region' of gephyrin (Prior et al., 1992). These studies, however, are complicated by the fact that the MogA domain forms trimers (Sola et al., 2001; Schwarz et al., 2001), while the C-terminal MoeA domain probably dimerizes in a manner similar to the *E. coli* MoeA protein (Schrag et al., 2001; Xiang et al., 2001). To define the regions involved in collybistin-gephyrin and GlyR β-gephyrin interactions, we used the GAL4 yeast two-hybrid system (Fields and Song, 1989). Full-length rat gephyrin (P1 isoform Prior et al., 1992) interacted readily with baits for $CB2_{SH3-}$ and the large intracellular loop of the human GlyR β subunit (Rees et al., 2003; Fig. 4*A*). N-terminal truncations of gephyrin lacking the MogA domain and the 'linker region' revealed normal interaction with the GlyR β-subunit bait (deletions 92, 184, 276, 305 and 323; Fig. 4*A*). The same gephyrin constructs, except deletion 323, also showed normal interaction with the $CB2_{SH3-}$ bait (Fig. 4*A,B*). This finding is significant, since the GlyR β bait shows a strong interaction with deletion 323, indicating that this gephyrin fragment is indeed expressed in yeast (Fig. 4*A,B*). Deletions at either end of the MoeA homology domain of gephyrin (deletions 336, 643, 674 or 704) abolished both $CB2_{SH3-}$ and GlyR β subunit interactions. A bait corresponding to the MoeA homology domain of gephyrin revealed that while deletions 305 and 323 showed strong MoeA-MoeA interactions (Fig. 4*B*), deletions 336, 643, 674 and 704 either impaired or abolished MoeA-MoeA multimerization.

Since deletions 305 and 323 appeared to demarcate a region important for collybistin-gephyrin interactions, we used an alanine mutation scan across this region to further define the amino acids involved. This revealed that mutants A4 and A5, which together span the short peptide sequence PFPLTSMDKA (Fig. 4*C,D*), disrupted collybistin-gephyrin interactions without affecting the

12

GlyR β-gephyrin interaction. It is noteworthy that the P-F-P motif at the beginning of the putative collybistin-binding motif is lost in the deletion construct 323 (Fig. 4D). Mutation of residues flanking the PFPLTSMDKA motif (mutants Geph-A3 and Geph-A6) did not affect collybistin-gephyrin or GlyR β-gephyrin interactions in yeast (Fig. 4C,D). To test whether the A4 and A5 alanine mutants disrupted collybistin-gephyrin co-localization in mammalian cells, we next introduced these mutations into pEGFP-gephyrin. These mutations were sufficient to either disrupt (EGFP-GephA4) or severely weaken (EGFP-GephA5) collybistin-gephyrin co-localization (Fig. 4E) upon co-expression with myc-CB2$_{SH3-}$ in HEK293 cells. In addition, submembrane targeting was abolished for both EGFP-A4 and EGFP-A5 (Fig. 4E).

Expression of EGFP-gephyrin in transfected cortical neurons resulted in punctate staining throughout dendritic processes (Fig. 5A), which co-localizes with staining for mAb7a (gephyrin) and GAD (Fig. 5E). However, when neurons were transfected with the EGFP-GephA4 mutant, dendritic puncta were dramatically reduced. Two main phenotypes were noted: either gephyrin accumulated in large aggregates in the cell soma (Fig. 5B) or cell soma plus dendrites (Fig. 5C). These gephyrin aggregates were no longer juxtaposed to GABAergic terminals (Fig. 5F,G). Therefore, EGFP-GephA4 acts as a dominant-negative factor trapping endogenous gephyrin and preventing proper apposition of presynaptic and postsynaptic structures. By contrast, mutant EGFP-GephA5 shows a few large dendritic clusters and appears to trap endogenous gephyrin at these sites (Fig. 5D,H). Quantitative analysis (Fig. 5I) demonstrated that the average endogenous gephyrin cluster number (mAb7a immunofluorescence) was reduced to 2 ± 1.95 clusters per 40 μm segment per cell for EGFP-GephA4 (n = 12 neurons) and 4.63 ± 2.01 clusters for EGFP-GephA5 per 40 μm segment per cell. These results were statistically significant when compared to EGFP-gephyrin, which showed an average of 9.77 ± 2.74 clusters per 40 μm segment per cell (n = 13 neurons; $p<0.001$, Student's t-test). In summary, both EGFP-GephA4 and EGFP-GephA5 mutants effectively interfere with clustering of endogenous gephyrin in transfected cortical

neurons. As in HEK293 cells (Fig. 4*E*), mutant EGFP-GephA4 is particularly effective, leading to a five-fold reduction of endogenous gephyrin clusters.

ARHGEF9 as a candidate gene for hyperekplexia

Hereditary hyperekplexia is a neurological disorder characterized by an excessive startle response, which can be caused by diverse dominant and recessive mutations in the genes encoding the GlyR α1 (*GLRA1*; Rees et al., 2001) or β subunits (*GLRB*; Rees et al., 2002). However, a significant portion of patients with hyperekplexia do not appear to have mutations in either *GLRA1* (Vergouwe et al., 1997) or *GLRB* (Rees et al., 2002) suggesting that other components of the GlyR signaling complex, such as gephyrin (*GPHN:* Rees et al., 2003) and collybistin (Gene symbol: *ARHGEF9*) may be involved. *ARHGEF9* consists of ten exons distributed over ~190 kb of human chromosome Xq22.1 (Table S1, Fig. 6*A*). Expressed sequence tag (EST) analysis revealed the existence of two alternative first exons (denoted exons 1a and 1b; Table S1), suggesting that *ARHGEF9* has two promoters that might control tissue-specific or developmentally-regulated changes in gene expression. Exon 1a encodes a long N-terminus (MQWIRGGSGM) while exon 1b encodes a shorter sequence (MTL). Exons 1a and 1b do not appear to influence utilization of exon 2, which encodes the SH3 domain (data not shown).

We used PCR (primers listed in Table S2) and automated dHPLC to detect *ARHGEF9* mutations and polymorphisms in a cohort of 32 hyperekplexia patients. Two single-nucleotide polymorphisms (SNP's) were detected in the intronic regions of exon 1b (IVS2 +43 t → c; het = 0.05) and exon 10 (IVS11 -64 t → c; het = 0.04) in both male and female patients and control cohorts. Significantly, a missense mutation (G164C) in the *ARHGEF9* coding region was discovered in one patient, which causes a glycine to alanine (G55A) substitution at position 55 of hPEM-2 (Fig. 6*B,C* and inset). The mutant genotype creates a *Nla*III restriction site (5'-GATG-3' to 5'-CATG-3'), a situation which was not detected in over two hundred unrelated Caucasian control chromosomes (e.g. Fig. 6*D*). A glycine residue is found at the equivalent position in 97% of known SH3 domains (2580/2669) as

assessed by using psiBLAST (http://www.biology.wustl.edu/gcg/psiblast.html) against the NCBI non-redundant database. A molecular model of the SH3 domain structure (Fig. 6*E*) shows that the G55A substitution lies in the middle of a β strand, and that this position of the protein backbone has Phi/Psi angles just beyond the limits of what is normally allowed for a non-glycine amino acid. G55A lies proximal to one of a series of residues that have been implicated in binding the proline-rich motif (Fig. 6*B*).

The patient was the first-born child of a 32-year-old woman, delivered in the 36th week of gestation. Immediately after delivery, cyanosis and muscular stiffness (suggestive of muscular hypertonia) were noted. The child also appeared to stare. During the following weeks, the child developed tonic seizures that were provoked by tactile stimulation. To counter the seizures, initially phenobarbital and then lamotrigene were administered. Although the latter treatment was initially effective, after 3½ months of age the seizures recurred and were often precipitated by extreme emotions. At four months of age a diagnosis of hyperekplexia was made, but therapy with clonazepam was unsuccessful. EEG monitoring coupled with ambulatory video revealed that the seizures were both hyperekplectic and epileptic in origin. During the following years, the child suffered from frequent long-lasting seizures, accompanied by the arrest and later decline of psychomotor development. Eventually, a progressive epileptic encephalopathy as well as hyperekplexia became evident and poly-drug treatment failed to provide adequate long-term seizure control. At four years of age the subject was severely retarded and suffered almost daily severe long-lasting fits both epileptic and non-epileptic in origin, eventually leading to death at the age of four years and four months.

Functional analysis of the G55A mutation

The clinical symptoms above are consistent with a mislocalization of neuronal gephyrin and associated glycine and $GABA_A$ receptors. We therefore assessed possible functional

consequences of the G55A mutation. Unlike myc-CB2$_{SH3+}$ (Fig. *1G*) or myc-CB3$_{SH3+}$ (Fig. *6F*), myc-CB3$_{SH3+}$G55A did not co-localize with large cytoplasmic EGFP-gephyrin aggregates in transfected HEK293 cells, but like myc-CB2$_{SH3-}$ (Fig. 1*I*), myc-CB3$_{SH3+}$G55A translocated gephyrin to submembrane microaggregates (Fig. *6G*). This result suggests that the G55A mutation disrupts the SH3 domain structure and/or function. In cortical neurons, 'wild-type' myc-CB3$_{SH3+}$ is diffusely expressed within the soma and proximal and distal dendrites and does not influence endogenous gephyrin clustering (Fig. *6H-J,Q*). The average gephyrin cluster number was 11.9 ± 4.44 per 40 μm dendritic segment (n = 11 neurons) for myc-CB3$_{SH3+}$. By contrast, myc-CB3$_{SH3+}$G55A forms a tight association with endogenous gephyrin and is confined to the cell soma and proximal dendrites, indicating a deficit in dendritic trafficking of this mutant protein (Fig. *6K-M*). In another subset of cells, myc-CB3$_{SH3+}$G55A is found in large somatic and dendritic aggregates (Fig. *6N-P*) which results in an almost complete loss of gephyrin clusters. Quantitative analysis of gephyrin clustering shows that expression of myc-CB3$_{SH3+}$G55A results in a dramatic loss of endogenous gephyrin clusters (Fig. 6Q). The average cluster number (mAb7a immunofluorescence) was reduced to 1.55 ± 0.72 clusters per 40 μm segment per cell for myc-CB3$_{SH3+}$G55A, which is statistically significant compared to myc-CB3$_{SH3+}$ (n = 11 cells per construct, p<0.001, Student's t-test).

In order to address possible functional consequences at inhibitory synapses we assessed whether transfection of myc-CB3$_{SH3+}$G55A would affect postsynaptic localization of GABA$_A$ receptors. Triple staining of neurons transfected with myc-CB3$_{SH3+}$ with antibodies specific for this construct, for GABA terminals (GAD) and for the GABA$_A$ receptor γ2 subunit revealed, as expected, diffuse distribution of this collybistin isoform and proper localization of GABA$_A$ receptors at postsynaptic sites (Fig. *7A-D*). Enlargement of a dendritic segment (Fig. *7E-H*) shows clear co-localization of GABA$_A$ receptors (red) and GAD (blue) resulting in purple puncta (arrows in Fig. *7H*). By contrast, in neurons transfected with myc-CB3$_{SH3+}$G55A, GABA$_A$ receptors were largely absent from the dendritic compartment (Fig. *7I-P*). Quantitative analysis

of $GABA_A$ receptor clustering (Fig. 7Q) shows that the average cluster number was reduced to 2.08 ± 1.29 clusters per 40 µm segment per cell for myc-CB3$_{SH3+}$G55A, which is statistically significant when compared to 10.04 ± 1.57 clusters for myc-CB3$_{SH3+}$ (n = 12 cells per construct, p<0.001, Student's t-test). This mislocalization of $GABA_A$ receptors, together with a corresponding expected deficit in glycine receptor trafficking in brain stem and spinal cord neurons, is likely to be causal for the clinical phenotype of the patient described above.

Discussion

The dendritic trafficking of receptors and clustering at appropriate sites in the postsynaptic membrane are extremely important events in the formation of functional synapses. This study reveals that the RhoGEF collybistin is a key molecule in regulating synaptic localization of gephyrin and by association, $GABA_A$ and glycine receptors. Firstly, we have reported the characterization of new variants of collybistin, which are created by alternative splicing of exons encoding an N-terminal *src* homology 3 (SH3) domain and three alternate C-termini (CB1, CB2 and CB3). Secondly, we have shown that the SH3 domain *negatively* regulates the ability of collybistin to translocate gephyrin to submembrane microaggregates in HEK293 cells. Since most endogenous collybistin isoforms harbor this region, this strongly suggests that collybistin activity is regulated by protein-protein interactions at the SH3 domain. Other functional domains of collybistin are also crucial, since gephyrin clustering requires both collybistin-gephyrin interactions and an intact collybistin PH domain. Thirdly, we have mapped the binding sites for collybistin and the GlyR β subunit on gephyrin to the C-terminal MoeA homology domain, and show that multimerization of the MoeA domain is a requirement for both collybistin-gephyrin and GlyR-gephyrin interactions. Lastly, we present the first significant *genetic* evidence that collybistin is important for the correct synaptic targeting of gephyrin: a G55A mutation in exon 2 of the human collybistin gene (*ARHGEF9*) results in symptoms of both hyperekplexia and epilepsy, which is likely to be caused by mislocalization of gephyrin and associated GlyR and $GABA_A$ receptors.

Functional significance of collybistin alternative splicing

In addition to the original rat collybistin isoforms (now denoted $CB1_{SH3+}$ and $CB2_{SH3-}$), we have cloned two additional isoforms ($CB2_{SH3+}$ and $CB3_{SH3+}$) from neonatal rat brain. We also determined that the CB2 and CB3 isoforms are of equal abundance in postnatal rat/mouse brain (CB1 was not detected), and that in adult human spinal cord and brain, $CB3_{SH3+}$ (but not CB1 or CB2) was detected. Alternative splicing of N- and C-terminal exons indicates that care must be applied in interpreting studies using *in situ* hybridization (Kins et al., 2000; Kneussel et al., 2001a) or when generating collybistin-specific antisera. The finding that $CB2_{SH3+}$ and $CB3_{SH3+}$ are functionally inactive in recombinant gephyrin clustering assays is a paradox, as the vast majority of spliced transcripts in rat, mouse and human spinal cord or brain clearly seem to encode these isoforms. It appears that collybistin activity is regulated via protein-protein interactions or post-translational modifications at the SH3 domain and that this mechanism only operates correctly in neurons. In this model, collybistin could be 'activated' at specific subcellular locations by an SH3-interacting ligand or 'trigger protein'.

Functional collybistin is required for dendritic clustering of gephyrin

By overexpressing recombinant collybistin isoforms and mutants in cortical neurons, we have demonstrated that collybistin is an essential molecule for dendritic gephyrin clustering and for appropriate trafficking of $GABA_A$ receptors to synapses. A similar role for collybistin is likely at glycinergic synapses of brainstem and spinal cord neurons. The distribution of epitope-tagged collybistin in neurons suggested that the protein is present at, but not limited to, synaptic sites. Analyses of the expression pattern of the PH domain deletion mutant, $CB2_{SH3-}\Delta PH$, suggested that collybistin is involved in dendritic transport of gephyrin to inhibitory synapses. Deletion of the PH domain resulted in accumulation of endogenous gephyrin in proximal dendrites and significantly reduced endogenous gephyrin clustering. Whether this mutation disrupts PH domain-membrane phosphoinositide interactions, or the binding of one or more key collybistin-interacting proteins remains to be determined. The RhoGEF domain deletion also disrupted

18

submembrane targeting of gephyrin; this is likely due to the fact that $CB2_{SH3-}\Delta RhoGEF$ no longer interacts with gephyrin, rather than deficits in GDP-GTP exchange.

Interaction of collybistin and GlyR β with gephyrin requires MoeA-MoeA interactions

A C-terminal fragment encompassing amino acids 305-736 of gephyrin displayed robust binding to collybistin and gephyrin, meaning that all of the N-terminal MogA homology domain (amino acids 16-169) and most of the intervening 'linker' region (amino acids 170-322) are dispensable for binding these molecules. Furthermore, our results with deletion constructs indicated that the binding site for GlyR β must reside entirely within the MoeA homology domain (amino acids 323-736). If the gephyrin MoeA homology domain forms an antiparallel dimer, like *E. coli* MoeA (Menéndez et al., 1997; Schrag et al., 2001; Xiang et al., 2001), our results strongly suggest that two equivalent GlyR β binding sites would be present at the MoeA-MoeA homology domain interface. Whether these two equivalent sites would bind a single GlyR heteromer, which is thought to contain two β subunits (stoichiometry $\alpha 1_3 \beta_2$) or two distinct receptor pentamers is presently unclear. Localization of the residues on gephyrin that interact with GlyRs will probably require co-crystallization of the MoeA homology domain with a peptide corresponding to the gephyrin-binding site on the GlyR β subunit (Kneussel et al., 1999a). Caution must be exercised with the analysis of mutants that 'disrupt' gephyrin-GlyR β subunit interactions, as these may simply be defective in MoeA-MoeA assembly. Ideally, a gephyrin mutant defective in GlyR β subunit binding would retain robust MoeA-MoeA interactions and would be translocated to submembrane microaggregates by collybistin.

A putative binding site for collybistin was located to the border of the 'linker' region and MoeA domain. Replacement of two adjacent groups of five amino acids either completely abolished (Geph-A4) or reduced (Geph-A5) collybistin-gephyrin interactions in HEK293 cells, but did not affect interaction with the GlyR β subunit. When expressed in cortical neurons, EGFP-gephyrin was localized at synaptic sites. This was evidenced by the almost perfect concordance of EGFP-

19

gephyrin fluorescence and mAb7a immunoreactivity, the latter representing both transfected and endogenous gephyrin and by the close apposition of EGFP-gephyrin and presynaptic immunoreactivity for GAD. In contrast, the gephyrin A4 and A5 mutants were both confined to large somatic and dendritic aggregates. These aggregates were not apposed to GAD immunoreactivity, indicating they were mislocalized. Quantitative analyses showed that punctate immunoreactivity for endogenous gephyrin in these transfected cells was severely reduced for EGFP-GephA4 and, to a lesser extent, for EGFP-GephA5. Interestingly, in cells expressing high levels of the EGFP-GephA4 mutant, the mutant and endogenous gephyrin proteins were both confined to large structures that extended far into peripheral dendrites. Thus, EGFP-GephA4 is effectively transported to peripheral dendrites although it cannot by itself interact with collybistin. Some collybistin dependent trafficking function may, however, be provided indirectly through multimerization of the mutant gephyrin construct with endogenous gephyrin which remains likely to interact with collybistin. By comparison, EGFP-GephA5 aggregates were smaller and more confined to the soma and proximal dendrites of transfected neurons. Our study identifies a critical sequence in gephyrin (PFPLTSMDKA) that appears to be essential for collybistin-gephyrin interactions and for normal collybistin-mediated trafficking and clustering of gephyrin to postsynaptic sites.

G55A mutation in the hPEM2 SH3 domain leads to hyperekplexia and epilepsy

The importance of collybistin for postsynaptic localization of gephyrin and associated ligand-gated chloride channels is underlined by the effect of the G55A mutation in the SH3 domain, leading to symptoms of both hyperekplexia and epilepsy. Recent studies (Douangmath et al., 2002; Groemping et al., 2003; Liu et al., 2003) have shown that there is sometimes binding of ligands to SH3 domains beyond the proline-rich peptide binding region. However, as the conserved glycine is buried within the SH3 domain structure, we consider that disrupting SH3 domain folding rather than the binding surface is the most probable mechanism of action. This is supported by studies in transfected HEK293 cells, revealing that the G55A mutation de-regulates

SH3 domain-containing collybistin isoforms, allowing translocation of gephyrin to submembrane sites in HEK293 cells. However, it is noteworthy that in neurons, myc-CB3$_{SH3+}$G55A differs dramatically from other recombinant collybistin isoforms, including myc-CB2$_{SH3-}$ which lacks the SH3 domain. CB3$_{SH3+}$G55A forms a tight association with gephyrin in dendritic clusters or forms large somatic and dendritic aggregates. These findings suggest that the G55A mutation causes a more complex deficit in dendritic trafficking of collybistin and/or disrupts collybistin-accessory protein interactions. The severe functional consequences of this mutation for the synaptic localization of gephyrin and, by association, GABA$_A$ receptors strongly suggests that the clinical phenotype observed in this patient was a consequence of the loss of gephyrin and major GABA$_A$ and GlyR subtypes from synaptic sites. While gene targeting experiments in mice have previously suggested that loss of gephyrin would be lethal in the first postnatal days, gephyrin is not only required for synaptic clustering of GABA$_A$ and GlyRs (Feng et al., 1998; Kneussel et al., 1999b, 2001b; Levi et al., 2004), but also for molybdoenzyme activity in non-neuronal tissues. Overall, we predict that mutations affecting collybistin function result in a 'neuronal' gephyrin phenotype, while peripheral molybdoenzyme-related functions of gephyrin are left undisturbed. The possibility remains that additional mutations in *ARHGEF9* may contribute to other cases of X-linked hyperekplexia and/or epilepsy.

References

Andrew M, Owen MJ (1997) Hyperekplexia: abnormal startle response due to glycine receptor mutations. Br J Psychiatry 170:106-108.

Bagrodia S, Taylor SJ, Jordon KA, Van Aelst L, Cerione RA (1998) A novel regulator of p21-activated kinases. J Biol Chem 273:23633-23636.

Douangamath A, Filipp FV, Klein AT, Barnett P, Zou P, Voorn-Brouwer T, Vega MC, Mayans OM, Sattler M, Distel B, Wilmanns M (2002) Topography for independent binding of alpha-helical and PPII-helical ligands to a peroxisomal SH3 domain. Mol Cell 10:1007-1017.

Dunne EL, Hosie AM, Wooltorton JR, Duguid IC, Harvey K, Moss SJ, Harvey RJ, Smart TG (2002) An N-terminal histidine regulates Zn^{2+} inhibition on the murine $GABA_A$ receptor $\beta3$ subunit. Br J Pharmacol 137:29-38.

Erickson JW, Cerione RA (2001) Multiple roles for Cdc42 in cell regulation. Curr Opin Cell Biol 13:153-157.

Essrich C, Lorez M, Benson JA, Fritschy JM, Lüscher B (1998) Postsynaptic clustering of major $GABA_A$ receptor subtypes requires the $\gamma2$ subunit and gephyrin. Nat Neurosci 1:563-571.

Feng G, Tintrup H, Kirsch J, Nichol MC, Kuhse J, Betz H, Sanes JR (1998) Dual requirement for gephyrin in glycine receptor clustering and molybdoenzyme activity. Science 282:1321-1324.

Fields S, Song O (1989) A novel genetic system to detect protein-protein interactions. Nature 340:245-246.

Fritschy JM, Mohler H (1995) $GABA_A$-receptor heterogeneity in the adult rat brain: differential regional and cellular distribution of seven major subunits. J Comp Neurol 359:154-194.

Fuhrmann JC, Kins S, Rostaing P, El Far O, Kirsch J, Sheng M, Triller A, Betz H, Kneussel, M (2002) Gephyrin interacts with dynein light chains 1 and 2, components of motor protein complexes. J Neurosci 22:5393-5402.

Fuller KJ, Morse MA, White JH, Dowell SJ, Sims MJ (1998) Development of a yeast trihybrid screen using stable yeast strains and regulated protein expression. Biotechniques 25:85-92.

Giesemann T, Schwarz G, Nawrotzki R, Berhorster K, Rothkegel M, Schluter K, Schrader N, Schindelin H, Mendel RR, Kirsch J, Jockusch BM (2003) Complex formation between the postsynaptic scaffolding protein gephyrin, profilin, and Mena: a possible link to the microfilament system. J Neurosci 23:8330-8339.

Groemping Y, Lapouge K, Smerdon SJ, Rittinger K (2003) Molecular basis of phosphorylation-induced activation of the NADPH oxidase. Cell 113:343-355.

Grosskreutz Y, Hermann A, Kins S, Fuhrmann JC, Betz H, Kneussel M (2001) Identification of a gephyrin-binding motif in the GDP/GTP exchange factor collybistin. Biol Chem 382:1455-1462.

Guex N, Peitsch MC (1997) SWISS-MODEL and the Swiss-PdbViewer: an environment for comparative protein modeling. Electrophoresis 18:2714-2723.

Habets GG, Scholtes EH, Zuydgeest D, van der Kammen RA, Stam JC, Berns A, Collard JG (1994) Identification of an invasion-inducing gene, Tiam-1, that encodes a protein with homology to GDP-GTP exchangers for Rho-like proteins. Cell 77:537-49.

Handford CA, Lynch JW, Baker E, Webb GC, Ford JH, Sutherland GR, Schofield PR (1996) The human glycine receptor β subunit: primary structure, functional characterisation and chromosomal localisation of the human and murine genes. Mol Brain Res 35:211-219.

Harvey RJ, Thomas P, James CH, Wilderspin A, Smart TG (1999) Identification of an inhibitory Zn^{2+} binding site on the human glycine receptor α1 subunit. J Physiol 520:53-64.

Karolchik D, Baertsch R, Diekhans M, Furey TS, Hinrichs A, Lu YT, Roskin KM, Schwartz M, Sugnet CW, Thomas J, Weber RJ, Haussler D, Kent WJ (2003) The UCSC Genome Browser Database. Nucl Acids Res 31:51-54.

Kavran JM, Klein DE, Lee A, Falasca M, Isakoff SJ, Skolnik EY, Lemmon MA (1998) Specificity and promiscuity in phosphoinositide binding by pleckstrin homology domains. J Biol Chem 273:30497-30508.

Kawasaki Y, Senda T, Ishidate T, Koyama R, Morishita T, Iwayama Y, Higuchi O, Akiyama T (2000) Asef, a link between the tumor suppressor APC and G-protein signaling. Science 289:1194-1197.

Kins S, Betz H, Kirsch J (2000) Collybistin, a newly identified brain-specific GEF, induces submembrane clustering of gephyrin. Nat Neurosci 3:22-29.

Kirsch J, Langosch D, Prior P, Littauer UZ, Schmitt B, Betz H (1991) The 93-kDa glycine receptor-associated protein binds to tubulin. J Biol Chem 266:22242-22245.

Kirsch J, Kuhse J, Betz H (1995) Targeting of glycine receptor subunits to gephyrin-rich domains in transfected human embryonic kidney cells. Mol Cell Neurosci 6:450-461.

Kneussel M, Betz H (2000) Clustering of inhibitory neurotransmitter receptors at developing postsynaptic sites, the membrane activation model. Trends Neurosci 23:429-435.

Kneussel M, Hermann A, Kirsch J, Betz H (1999a) Hydrophobic interactions mediate binding of the glycine receptor β-subunit to gephyrin. J Neurochem 72:1323-1326.

Kneussel M, Brandstatter JH, Laube B, Stahl S, Müller U, Betz H (1999b) Loss of postsynaptic GABA$_A$ receptor clustering in gephyrin deficient mice. J Neurosci 19:9289-9297.

Kneussel M, Engelkamp D, Betz H (2001a) Distribution of transcripts for the brain-specific GDP/GTP exchange factor collybistin in the developing mouse brain. Eur J Neurosci 13:487-492.

Kneussel M, Brandstatter JH, Gasnier B, Feng G, Sanes JR, Betz H (2001b) Gephyrin-independent clustering of postsynaptic GABA$_A$ receptor subtypes. Mol Cell Neurosci 17:973-982.

Levi S, Logan SM, Tovar KR, Craig AM (2004) Gephyrin is critical for glycine receptor clustering but not for the formation of functional GABAergic synapses in hippocampal neurons. J Neurosci 24:207-217.

Liu Q, Berry D, Nash P, Pawson T, McGlade CJ, Li SS (2003) Structural basis for specific binding of the Gads SH3 domain to an RxxK motif-containing SLP-76 peptide: a novel mode of peptide recognition. Mol Cell 11:471-481.

Mackay DJ, Hall A (1998) Rho GTPases. J Biol Chem 273:20685-20688.

Mammoto A, Sasaki T, Asakura T, Hotta I, Imamura H, Takahashi K, Matsuura Y, Shirao T, Takai Y (1998) Interactions of drebrin and gephyrin with profilin. Biochem Biophys Res Commun 243:86-89.

Manser E, Loo TH, Koh CG, Zhao ZS, Chen XQ, Tan L, Tan I, Leung T, Lim L (1998) PAK kinases are directly coupled to the PIX family of nucleotide exchange factors. Mol Cell 1:183-192.

Meier J, De Chaldee M, Triller A, Vannier C (2000) Functional heterogeneity of gephyrins. Mol Cell Neurosci 16:566-577.

Menéndez C, Otto A, Igloi G, Nick P, Brandsch R, Schubach B, Bottcher B, Brandsch R (1997) Molybdate-uptake genes and molybdopterin-biosynthesis genes on a bacterial plasmid--characterization of MoeA as a filament-forming protein with adenosine triphosphatase activity. Eur J Biochem 250:524-531.

Prior P, Schmitt B, Grenningloh G, Pribilla I, Multhaup G, Beyreuther K, Maulet Y, Werner P, Langosch D, Kirsch J and Betz H (1992) Primary structure and alternative splice variants of gephyrin, a putative glycine receptor-tubulin linker protein. Neuron 8:1161-1170.

Rees MI, Lewis TM, Vafa B, Ferrie C, Corry P, Muntoni F, Jungbluth H, Stephenson JB, Kerr M, Snell RG, Schofield PR, Owen MJ (2001) Compound heterozygosity and nonsense mutations in the α1 subunit of the inhibitory glycine receptor in hyperekplexia. Hum Genet 109:267-270.

Rees MI, Lewis TM, Kwok JB, Mortier GR, Govaert P, Snell RG, Schofield PR, Owen MJ (2002) Hyperekplexia associated with compound heterozygote mutations in the β subunit of the human inhibitory glycine receptor (GLRB). Hum Mol Genet 11:853-860.

Rees MI, Harvey K, Ward H, White JH, Evans IL, Duguid IC, Hsu CCH, Coleman SL, Baer K, Waldvogel H, Gibbon F, Smart TG, Owen MJ, Harvey RJ, Snell RG (2003) Isoform heterogeneity of the human gephyrin gene (GPHN), binding domains to the glycine receptor and mutation analysis on hyperekplexia. J Biol Chem 278:24688-24696.

Reid T, Bathoorn A, Ahmadian MR, Collard JG (1999) Identification and characterization of hPEM-2, a guanine nucleotide exchange factor specific for Cdc42. J Biol Chem 274:33587-33593.

Sabatini DM, Barrow RK, Blackshaw S, Burnett PE, Lai MM, Field ME, Bahr BA, Kirsch J, Betz H, Snyder SH (1999) Interaction of RAFT-1 with gephyrin required for rapamycin-sensitive signaling. Science 284:1161-1164.

Schmitt B, Knaus P, Becker C-M, Betz H (1987) The M_r 93,000 polypeptide of the postsynaptic glycine receptor complex is a peripheral membrane protein. Biochemistry 26:805-811.

Schrag JD, Huang W, Sivaraman J, Smith C, Plamondon J, Larocque R, Matte A, Cygler M (2001) The crystal structure of Escherichia coli MoeA, a protein from the molybdopterin synthesis pathway. J Mol Biol 310:419-431.

Schwarz G, Schrader N, Mendel RR, Hecht HJ, Schindelin H (2001) Crystal structures of human gephyrin and plant Cnx1 G domains: comparative analysis and functional implications. J Mol Biol 312:405-418.

Schweizer C, Balsiger S, Bluethmann H, Mansuy IM, Fritschy JM, Mohler H, Lüscher B (2003) The γ2 subunit of GABA$_A$ receptors is required for maintenance of receptors at mature synapses. Mol Cell Neurosci 24:442-450.

Sola M, Kneussel M, Heck IS, Betz H, Weissenhorn W (2001) X-ray crystal structure of the trimeric N-terminal domain of gephyrin. J Biol Chem 276:25294-25301.

Triller A, Cluzeaud F, Pfeiffer F, Betz H, Korn H (1985) Distribution of glycine receptors at central synapses: an immunoelectron microscopy study. J Cell Biol 101:683-688.

Vergouwe MN, Tijssen MA, Shiang R, van Dijk JG, al Shahwan S, Ophoff RA, Frants RR (1997) Hyperekplexia-like syndromes without mutations in the GLRA1 gene. Clin Neurol Neurosurg 99:172-178.

Wherlock M, Mellor H (2002) The Rho GTPase family: a Racs to Wrchs story. J Cell Sci 115:239-240.

Worthylake DK, Rossman KL, Sondek J (2000) Crystal structure of Rac1 in complex with the guanine nucleotide exchange region of Tiam1. Nature 408:682-688.

Xiang S, Nichols J, Rajagopalan KV, Schindelin H (2001) The crystal structure of Escherichia coli MoeA and its relationship to the multifunctional protein gephyrin. Structure 9:299-310.

Figure Legends

Figure 1. Alternative splicing of rat and human collybistin mRNAs. Three different collybistin C-termini can be specified in the rat by the use of different cassette exons. For example, the CB2 (VTQRKWHY*) C-terminus is generated by insertion of a 62 bp exon (white lettering on black background; *A*). When omitted, an alternative C-terminus is specified (CB3) that is virtually identical to the C-terminus of human collybistin (hPEM-2). RT-PCR analysis shows that the exon encoding the N-terminal SH3 domain (*B*) is utilized in most rodent and human collybistin mRNAs (○ SH3+; □ SH3-). For C-terminal exons (*C*) both CB2 (○) and CB3 (□) are common in rodents, but only CB3 transcripts are evident in humans. Schematic diagram of the primary structures of known collybistin isoforms (*D*). Sequences encoding the SH3, RhoGEF and PH domains in the collybistin isoforms are indicated by grey boxes, and the different C-termini are indicated by white (CB1), black (CB2) or grey (CB3) boxes. Expression of myc-tagged CB2$_{SH3-}$ in HEK293 cells (*E*). Co-transfection of a plasmid construct encoding EGFP-gephyrin results in the formation of cytoplasmic aggregates (*F*), to which myc-CB2$_{SH3+}$ targets (*G*). However, co-expression of EGFP-gephyrin with the CB2 variant lacking the SH3 domain (myc-CB2$_{SH3-}$) results in a redistribution of EGFP-gephyrin and collybistin to submembrane microaggregates (*H,I*). Scale bar = 10 μm. Note that panels E-G are single Z-plane confocal images, while H and I are Z-stacks at the cell surface.

Figure 2. A DsRed-GlyR β fusion protein is efficiently targeted to EGFP-gephyrin aggregates in HEK293 cells. Z-stack confocal images showing triple transfection of HEK293 cells with plasmid constructs encoding a DsRed-GlyR β subunit intracellular loop fusion protein (*A*; DsRed-GlyR β), EGFP-gephyrin (*B*) and myc-CB2$_{SH3-}$ (*C*). Note that DsRed-GlyR β is readily trapped by EGFP-gephyrin submembrane clusters, while myc-CB2$_{SH3-}$ has a more diffuse distribution pattern throughout the cytoplasm (*D*). Scale bar = 10 μm.

Figure 3. Functional collybistin is required for accumulation of gephyrin in dendritic clusters. Expression of myc-tagged CB2$_{SH3-}$ (*A,C*) and CB2$_{SH3+}$ (*B,D*) isoforms in transfected mouse cortical neurons reveals a diffuse distribution throughout the cell soma and dendrites (see enlargements in *C,D*) without affecting gephyrin cluster number (*E*; values are mean ± s.e.). Constructs lacking the RhoGEF or PH domains (*inset*) were co-expressed with EGFP-gephyrin in HEK293 cells. Single Z-plane confocal images show that myc-CB2$_{SH3-}$ΔRhoGEF mutant no longer co-localizes with EGFP-gephyrin and prevents submembrane targeting (*F,G*). By contrast, the myc-CB2$_{SH3-}$ΔPH mutant co-localizes with EGFP-gephyrin, but also results in the production of cytoplasmic collybistin-gephyrin microclusters (*H,I*). Note that gephyrin and collybistin aggregates in *F-I* are *intracellular*, since the cell nucleus is clearly visible in each single optical section. In transfected mouse cortical neurons, myc-CB2$_{SH3-}$ΔPH acts as a dominant-negative factor, competing with endogenous collybistin for binding sites on gephyrin (*J,K*). Quantitative analysis of mAb7a staining indicates a statistically significant loss of dendritic gephyrin clusters (*E;* * p<0.001, Student's t-test, n = 10 to 11 cells per construct) and accumulation of endogenous gephyrin in aggregates in the proximal dendrites (white arrowheads). Scale bars = 22 μm (*A,B*), 11 μm (*C,D*), 5 μm (*F-I*), 23 μm (*H*) and 11.5 μm (*K*).

Figure 4. Mapping of the collybistin binding site on gephyrin. Deletion constructs of the rat gephyrin P1 isoform in pACT2 (Clontech) were tested using the GlyR β subunit intracellular loop (β) and full-length collybistin CB2$_{SH3-}$ isoform (CB2) as baits (*A*). Both proteins interact with full-length gephyrin in yeast, as judged by a semiquantitative LacZ assay (+++ strong interaction, + weak interaction, ---, no interaction). Deletion analysis indicated that the gephyrin MogA domain (MogA) and most of the 'linker region' do not appear to contribute to either GlyR β subunit or collybistin binding. Deletions into the gephyrin MoeA domain (MoeA) destroy interactions with both collybistin and the GlyR β subunit, due to the loss of MoeA-MoeA domain interactions. Geph-305 interacts with GlyR β, CB2$_{SH3-}$ and MoeA domain baits, whereas Geph-323 (which corresponds to a MoeA domain prey) interacts with GlyR β and MoeA, but not

CB2$_{SH3-}$(*B*). Mutants (Geph-A1 to Geph-A7) which span the Geph-305 to Geph 323 region were then constructed and tested in yeast assays (*C,D*). Mutations Geph-A4 and Geph-A5 (boxed) abolished interactions with CB2$_{SH3-}$, but not the GlyR β subunit (*C,D*). The corresponding mutants in EGFP-gephyrin eliminated (EGFP-GephA4) or weakened (EGFP-GephA5) co-localization with myc-CB2$_{SH3-}$ (*E*) and blocked submembrane microaggregate formation. Scale bar = 10 μm.

Figure 5. Disruption of the collybistin binding site on gephyrin prevents accumulation of gephyrin at postsynaptic sites. EGFP-tagged gephyrin (*A,E*) and the mutants EGFP-GephA4 (*B,C,F,G*) and EGFP-GephA5 (*D,H*) were transfected into cortical neurons and the cells immunostained for gephyrin (mAb7a, *A-D*) or GAD (mAbGAD-6, *E-H*). Two examples of cells are shown for EGFP-GephA4 representing comparatively low (*B,F*) and high (*C,G*) levels of expression and corresponding aggregate phenotypes. Note the perfect colocalization of transfected EGFP-gephyrin with endogenous gephyrin in yellow puncta (*A*). The few remaining red puncta indicate endogenous gephyrin expressed on dendrites of non-transfected neighbouring cells that are therefore not colocalized with EGFP-gephyrin. EGFP-gephyrin is localized at postsynaptic sites juxtaposed to presynaptic GAD (*E*, arrows). Mutants EGFP-GephA4 and EGFP-GephA5 form large aggregates in the soma and/or dendrites, which are no longer juxtaposed to GABAergic terminals (*F-H*). Endogenous gephyrin has been trapped in these extrasynaptic gephyrin mutant aggregates, which therefore appear yellow (*B-D*). Quantitative analysis of mAb7a staining indicates a statistically significant loss of synaptic gephyrin clusters (*I;* * p<0.001, Student's t-test, n = 12 to 13 cells per construct) for the EGFP-GephA4 and EGFP-GephA5 mutants compared to EGFP-gephyrin. Scale bar = 20 μm.

Figure 6. Mutation of G55A in a patient with hyperekplexia and epilepsy

Genomic structure of the human collybistin gene (*ARHGEF9*) encoding hPEM-2 (*A*). The location of the mutation G55A (red lettering) in the N-terminal SH3 domain (underlined) of
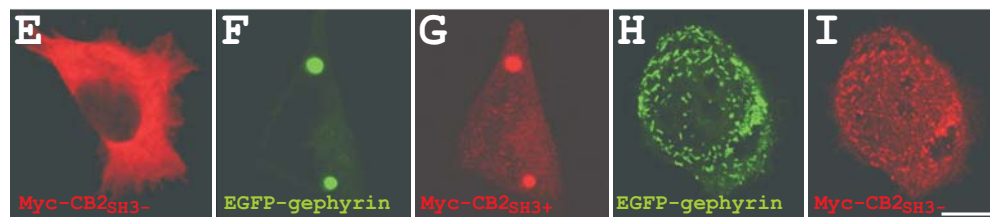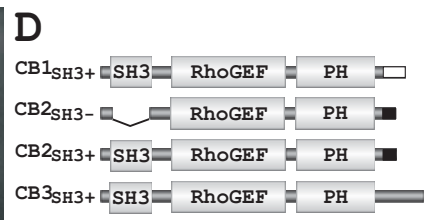
hPEM-2 is shown (*B*). G55A lies proximal to one of the series of residues that have been proposed to bind proline-rich motifs (blue lettering). DNA sequencing of exon 2 samples revealed a G to C substitution at position 164 of the collybistin coding sequence, causing a G55A missense mutation in the N-terminal SH3 domain of hPEM2 (*C*). G164; control sample; G164+G164C: ad-mixture of the patient sample with a female DNA control; G164C: G164C mutation. RFLP analysis of the G55A mutation: the G164C mutation creates a novel *Nla*III site at position 207 of the 313 bp exon 2 PCR fragment (*D*). This, in conjunction with another *Nla*III site at position 106, generates convergent fragments of 106 bp, 101 bp and 106 bp in the patient DNA sample (denoted P). Normal controls (C1-C4) have fragments of 207 and 106 bp. A molecular model (*E*) showing the location of G55 in the SH3 domain structure calculated with Swiss-Model (Guex and Petisch 1997). Confocal images showing HEK293 cells transfected with plasmid constructs for myc-CB3$_{SH3+}$ and EGFP-gephyrin (*F*) or myc-CB3$_{SH3+}$G55A and EGFP-gephyrin (*G*). Note that myc-CB3$_{SH3+}$ co-localizes with cytoplasmic EGFP-gephyrin aggregates, while myc-CB3$_{SH3+}$G55A results in submembrane microclusters of EGFP-gephyrin. Confocal images showing myc-CB3$_{SH3+}$ (*H-J*) and myc-CB3$_{SH3+}$G55A (*K-P*) expressed in cultured cortical neurons. Whereas wild-type myc-CB3$_{SH3+}$ (*H*) is expressed throughout the cell soma and dendrites and does not disrupt gephyrin localization (*H-J*), myc-CB3$_{SH3+}$G55A forms a tight association with endogenous gephyrin in clusters confined to proximal dendrites (*K-M)*. In a subset of transfected cells (*N-P*) myc-CB3$_{SH3+}$G55A forms large somatic and dendritic aggregates, which results in an almost complete loss of gephyrin clusters. Remaining red puncta in panels *I, L* and *O* represent gephyrin clusters from non-transfected cells in the same culture. Quantitative analysis of mAb7a immunofluorescence (*Q*) indicates a dramatic loss of gephyrin clusters (* $p<0.001$, Student's t-test, $n = 11$ cells per construct) for myc-CB3$_{SH3+}$G55A mutant compared to myc-CB3$_{SH3+}$. Scale bars = 10 μm (*F,G*), 35 μm (*H-P*).

Figure 7. Collybistin mutant CB3$_{SH3+}$G55A results in loss of GABA$_A$ receptor clusters

Triple staining of neurons transfected with either myc-CB3$_{SH3+}$ (*A-H*) or myc-CB3$_{SH3+}$G55A (*I-P*) with antibodies against the GABA$_A$ receptor γ2 subunits (red), myc tag (green) and GAD (blue). Note that in myc-CB3$_{SH3+}$-transfected neurons (*A-D*) GABA$_A$ receptor clusters are juxtaposed to GAD-positive terminals (a selected dendritic region is enlarged in images E-H). Overlap of GABA$_A$ receptor and GAD immunoreactivity appears pink in the merged image (arrows in *H*). By contrast, in neurons expressing myc-CB3$_{SH3+}$G55A, GABA$_A$ receptor immunoreactivity is largely confined to the cell soma (*I,M*), and large collybistin aggregates (*J,N*) are observed throughout the dendrites. Notably, these collybistin aggregates are not juxtaposed to GABAergic terminals (*K,L,O,P*). Quantitative analysis of γ2 subunit immunofluorescence (*Q*) indicates a statistically significant loss of GABA$_A$ receptor clusters (* $p<0.001$, Student's t-test, n = 12 cells per construct) for the myc-CB3$_{SH3+}$G55A mutant compared to myc-CB3$_{SH3+}$. Scale bars = 25 μm (*A-D, I-L*), 12.5 μm (*E-H, M-P*).

A

| rCB2 | M T V R K A S K Q K | V T Q R K W H Y * |
| rCB2 cDNA | aatgactgtgagaaaagcgtctaaacagaaag | taacccaaagaaaatggcactattagcc |

hPEM2		G V N S A R S V P
rCB3		G V N S A R S V P
rCB2 cDNA	cctgttccaggttaagaaactgaaaacactcaag	gtgtcaactctgctcgctcagttcca

hPEM2	P S Y P P P Q D P L N H G Q Y L V P D G
rCB3	P S Y P P P Q D P L N Q G Q Y L V P D G
rCB2 cDNA	ccttcctatccaccaccacaggacccgttaaaccagggccagtacctggtccccgatggc

hPEM2	I A Q S Q V F E F T E P K R S Q S P F W
rCB3	I A Q S Q V F E F T E P K R S Q S P F W
rCB2 cDNA	atcgctcagtctcaagtgtttgagttcactgaaccgaaacgcagccagtcaccattctgg

hPEM2	Q N F S R L T P F K K *
rCB3	Q N F S R L T P F K K *
rCB2 cDNA	caaaacttcagtaggttaaccccctcaaaaaataataacctataggaaggcagataattt

A — DsRed-GlyR β

B — EGFP-gephyrin

C — Myc-CB2$_{SH3-}$

D — Merge

A Gephyrin Myc-CB2$_{SH3-}$

B Gephyrin Myc-CB2$_{SH3+}$

C

D

E

CB2$_{SH3-}$ ΔRhoGEF

CB2$_{SH3-}$ ΔPH

PH

RhoGEF

F Myc-CB2$_{SH3-}$ΔRhoGEF

G EGFP-gephyrin

H Myc-CB2$_{SH3-}$ΔPH

I EGFP-gephyrin

J Gephyrin Myc-CB2$_{SH3-}$ΔPH

K

A

Panel A scale: 100 200 300 400 500 600 700

16   169   323   736

| MogA | Linker | MoeA |

Constructs:

		CB2	β	
1		+++	+++	
92		+++	+++	
184		+++	+++	
276		+++	+++	
368		---	---	
460		---	---	
552		---	---	MoeA
305		+++	+++	+++
323		---	+++	+++
336		---	---	+
305	643	---	---	---
305	674	---	---	---
305	704	---	---	+

B

	Geph305	Geph323
CB2		
β		
MoeA		

C

	GephA3	GephA4	GephA5	GephA6
CB2				
β				

D

```
MoeA                    MEFTTGLMSLDTALNEMLSRVTP   CB2   β
Geph-305  SAVDITKVARRHRMSPFPLTSMDKAFITVLEMTPV    +++   +++
Geph-323               LTSMDKAFITVLEMTPV          ---   +++

          <-----linker------>
                            ------MoeA------>
Geph-A1   AAAAATKVARRHRMSPFPLTSMDKAFITVLEMTPV    +++   +++
Geph-A2   SAVDIAAAAARHRMSPFPLTSMDKAFITVLEMTPV    +++   +++
Geph-A3   SAVDITKVARAAAAAPFPLTSMDKAFITVLEMTPV    +++   +++
Geph-A4   SAVDITKVARRHRMSAAAAASMDKAFITVLEMTPV    ---   +++
Geph-A5   SAVDITKVARRHRMSPFPLTAAAAAFITVLEMTPV    ---   +++
Geph-A6   SAVDITKVARRHRMSPFPLTSMDKAAAAAAEMTPV    +++   +++
Geph-A7   SAVDITKVARRHRMSPFPLTSMDKAFITVLAAAAA    +++   +++
```

E

Myc-CB2_{SH3-}   EGFP-GephA4   Myc-CB2_{SH3-}   EGFP-GephA5

A Gephyrin
   EGFP-gephyrin

B Gephyrin
   EGFP-GephA4

C Gephyrin
   EGFP-GephA4

D Gephyrin
   EGFP-GephA5

E GAD
   EGFP-gephyrin

F GAD
   EGFP-GephA4

G GAD
   EGFP-GephA4

H GAD
   EGFP-GephA5

I

EGFP-gephyrin
EGFP-GephA4
EGFP-GephA5

A

1A 1B 2 3 4 ——10kb 5 6 7 8 9 10

B

hPEM2: MTLLITGDSIVSAEAVWDHVTMANRELAFKAGDVIKVLDASNKDWWWGQIDDEEGWFPASFVRLWVNQE

G55A: MTLLITGDSIVSAEAVWDHVTMANRELAFKAGDVIKVLDASNKDWWWGQIDDEEAWFPASFVRLWVNQE

C

ATGAGGAGG**G**ATGGTTTC
G164

ATGAGGAGG**N**ATGGTTTC
G164+
G164C

ATGAGGAGG**C**ATGGTTTC
G164C

D

C1 C2 C3 C4 P M

CB3$_{SH3+}$ [SH3]—[RhoGEF]—[PH]

CB3$_{SH3+}$
G55A [SH3]—[RhoGEF]—[PH]
  G55A

E

F Myc-CB3$_{SH3+}$
EGFP-gephyrin

G Myc-CB3$_{SH3+}$G55A
EGFP-gephyrin

H Myc-CB3$_{SH3+}$

I Gephyrin

J Merge

K Myc-CB3$_{SH3+}$G55A

L Gephyrin

M Merge

N Myc-CB3$_{SH3+}$G55A

O Gephyrin

P Merge

Q

mAb7A puncta per dendritic segment

16
14
12
10
8
6
4
2

*

CB3$_{SH3+}$
CB3$_{SH3+}$G55A

A GABA_AR γ2   B Myc-CB3_{SH3+}   C GAD   D Merge

E   F   G   H

I GABA_AR γ2   J Myc-CB3_{SH3+}G55A   K GAD   L Merge

M   N   O   P

Q
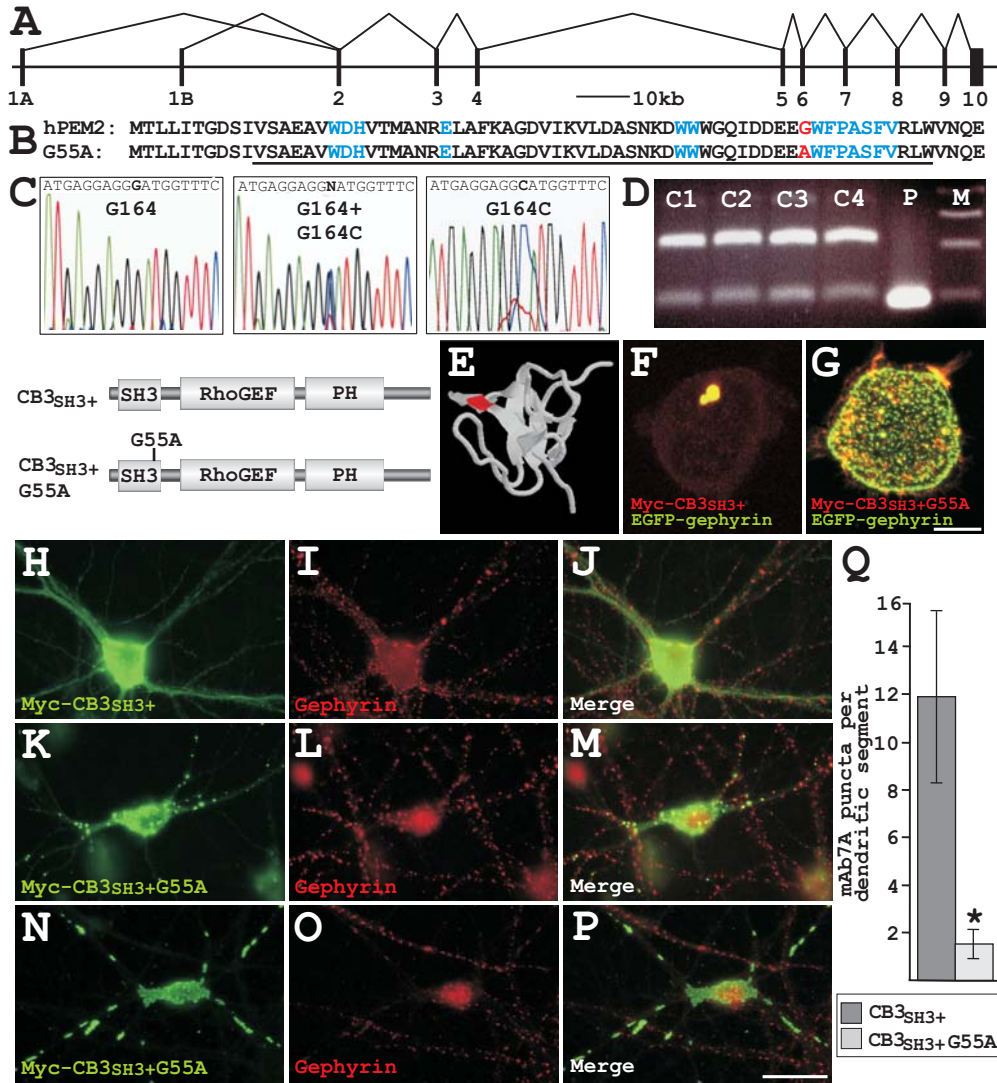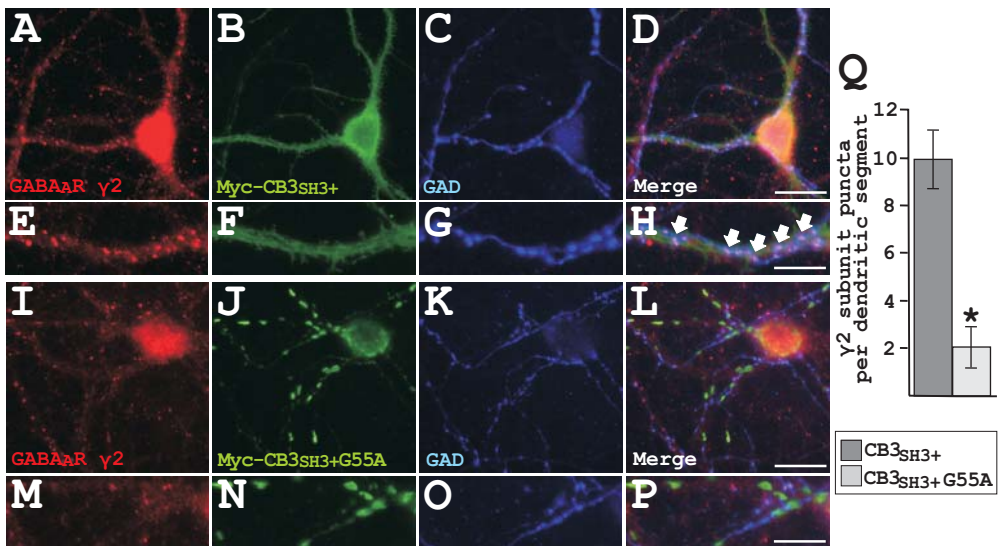
Supplementary data

The GDP-GTP exchange factor collybistin: an essential determinant of neuronal gephyrin clustering by Harvey et al.

```
                                                       SH3 domain
rCB1SH3+  MQWIRGGSGMLITGDSIVSAEAVWDHVTMANRELAFKAGDVIKVLDASNK 50
rCB2SH3+  MQWIRGGSGMLITGDSIVSAEAVWDHVTMANRELAFKAGDVIKVLDASNK 50
rCB3SH3+  MQWIRGGSGMLITGDSIVSAEAVWDHVTMANRELAFKAGDVIKVLDASNK 50
hPEM2           MTLLITGDSIVSAEAVWDHVTMANRELAFKAGDVIKVLDASNK 43
                 ----------------------------------------------

rCB1SH3+  DWWWGQIDDEEGWFPASFVRLWVNQEDGVEEGPSDVQNGHLDPNSDCLCL 100
rCB2SH3+  DWWWGQIDDEEGWFPASFVRLWVNQEDGVEEGPSDVQNGHLDPNSDCLCL 100
rCB3SH3+  DWWWGQIDDEEGWFPASFVRLWVNQEDGVEEGPSDVQNGHLDPNSDCLCL 100
hPEM2     DWWWGQIDDEEGWFPASFVRLWVNQEDEVEEGPSDVQNGHLDPNSDCLCL 93
           --------------------------------

rCB1SH3+  GRPLQNRDQMRANVINEIMSTERHYIKHLKDICEGYLKQCRKRRDMFSDE 150
rCB2SH3+  GRPLQNRDQMRANVINEIMSTERHYIKHLKDICEGYLKQCRKRRDMFSDE 150
rCB3SH3+  GRPLQNRDQMRANVINEIMSTERHYIKHLKDICEGYLKQCRKRRDMFSDE 150
hPEM2     GRPLQNRDQMRANVINEIMSTERHYIKHLKDICEGYLKQCRKRRDMFSDE 143

rCB1SH3+  QLKVIFGNIEDIYRFQMGFVRDLEKQYNNDDPHLSEIGPCFLEHQDGFWI 200
rCB2SH3+  QLKVIFGNIEDIYRFQMGFVRDLEKQYNNDDPHLSEIGPCFLEHQDGFWI 200
rCB3SH3+  QLKVIFGNIEDIYRFQMGFVRDLEKQYNNDDPHLSEIGPCFLEHQDGFWI 200
hPEM2     QLKVIFGNIEDIYRFQMGFVRDLEKQYNNDDPHLSEIGPCFLEHQDGFWI 193
                                      RhoGEF domain
rCB1SH3+  YSEYCNNHLDACMELSKLMKDSRYQHFFEACRLLQQMIDIAIDGFLLTPV 250
rCB2SH3+  YSEYCNNHLDACMELSKLMKDSRYQHFFEACRLLQQMIDIAIDGFLLTPV 250
rCB3SH3+  YSEYCNNHLDACMELSKLMKDSRYQHFFEACRLLQQMIDIAIDGFLLTPV 250
hPEM2     YSEYCNNHLDACMELSKLMKDSRYQHFFEACRLLQQMIDIAIDGFLLTPV 243

rCB1SH3+  QKICKYPLQLAELLKYTAQDHSDYRYVAAALAVMRNVTQQINERKRRLEN 300
rCB2SH3+  QKICKYPLQLAELLKYTAQDHSDYRYVAAALAVMRNVTQQINERKRRLEN 300
rCB3SH3+  QKICKYPLQLAELLKYTAQDHSDYRYVAAALAVMRNVTQQINERKRRLEN 300
hPEM2     QKICKYPLQLAELLKYTAQDHSDYRYVAAALAVMRNVTQQINERKRRLEN 293

rCB1SH3+  IDKIAQWQASVLDWEGDDILDRSSELIYTGEMAWIYQPYGRNQQRVFFLF 350
rCB2SH3+  IDKIAQWQASVLDWEGDDILDRSSELIYTGEMAWIYQPYGRNQQRVFFLF 350
rCB3SH3+  IDKIAQWQASVLDWEGDDILDRSSELIYTGEMAWIYQPYGRNQQRVFFLF 350
hPEM2     IDKIAQWQASVLDWEGEDILDRSSELIYTGEMAWIYQPYGRNQQRVFFLF 343
                          PH domain
rCB1SH3+  DHQMVLCKKDLIRRDILYYKGRIDMDKYEVIDIEDGRDDDFNVSMKNAFK 400
rCB2SH3+  DHQMVLCKKDLIRRDILYYKGRIDMDKYEVIDIEDGRDDDFNVSMKNAFK 400
rCB3SH3+  DHQMVLCKKDLIRRDILYYKGRIDMDKYEVIDIEDGRDDDFNVSMKNAFK 400
hPEM2     DHQMVLCKKDLIRRDILYYKGRIDMDKYEVVDIEDGRDDDFNVSMKNAFK 393

rCB1SH3+  LHNKETEEVHLFFAKKLEEKIRWLRAFREERKMVQEDEKIGFEISENQKR 450
rCB2SH3+  LHNKETEEVHLFFAKKLEEKIRWLRAFREERKMVQEDEKIGFEISENQKR 450
rCB3SH3+  LHNKETEEVHLFFAKKLEEKIRWLRAFREERKMVQEDEKIGFEISENQKR 450
hPEM2     LHNKETEEIHLFFAKKLEEKIRWLRAFREERKMVQEDEKIGFEISENQKR 443

rCB1SH3+  QAAMTVRKASKQKGRVGEEENQSLELKRACEVLQRLWSPGKKS         493
rCB2SH3+  QAAMTVRKASKQKVTQRKWHY                              471
rCB3SH3+  QAAMTVRKASKQKGVNSARSVPPSYPPPQDPLNQGQYLVPDGIAQSQVFE 500
hPEM2     QAAMTVRKVPKQKGVNSARSVPPSYPPPQDPLNHGQYLVPDGIAQSQVFE 493

rCB3SH3+  FTEPKRSQSPFWQNFSRLTPFKK                            523
hPEM2     FTEPKRSQSPFWQNFSRLTPFKK                            516
```

Figure S1. Alignment of rat collybistin isoforms with the human homologue. The amino acid sequences of the rat $CB1_{SH3+}$, $CB2_{SH3+}$ and $CB3_{SH3+}$ isoforms were aligned with human collybistin (hPEM2) using the computer program PILEUP (Wisconsin Sequence Analysis package, Version 8, Genetics Computer Group, Madison, WI). Positions at which rat collybistins differ from hPEM2 are indicated by bold lettering. The positions of the src-homology 3 (SH3), RhoGEF and pleckstrin homology (PH) domains are indicated by open boxes. The different C-termini of the rat collybistin isoforms, which are generated by alternative splicing, are indicated by grey shading.

Table 1. Structure of the human collybistin gene (ARHGEF9)

Exon	Encoding	Exon	Acceptor	Donor	Intron
1a	5' UTR + 'MQW' N-terminus	†212		GGAATGgtgagt	60404
1b	5' UTR + 'MTL' N-terminus	†807		ACGTTGgtatat	29592
2	SH3 domain	180	cctaagCTGAT	GTGAGGgtgagt	18082
3	Gephyrin BD + RhoGEF	192	ccacagCTCTG	TGTGAGgtaacc	8953
4	RhoGEF domain	180	ctacagGGCTA	GAGCACgtaagt	58000*
5	RhoGEF domain	233	ccacagCCAGA	CCACAGgtaagg	4172
6	RhoGEF + linker	130	tcacagTGACT	TGGGAGgtagga	8020
7	linker + PH	132	tcccagGGCGA	AAGAAGgtaacc	10148
8	PH domain	244	atctagGACCT	AAATTGgtaagt	11445
9	linker	69	ttttagGCTTT	AAAAAGgtaaag	5770
10	CB3 C-terminus and 3'UTR	3242	ctctagGTGTC		

*Estimated intron size
†Minimum exon size

Table 2. Primers for ARHGEF9 analysis

Exon	Amplicon	Forward primer	Reverse primer
1a	332 bp	5'-GGAGAGACAGAGCCTGCCG-3'	5'-AGGGTGCTCACTGCCTTGT-3'
1b	579 bp	5'-CAGCTAGGGCACAACGATCAG-3'	5'-CTATACGCGCAGGCATTCTTA-3'
2	313 bp	5'-AAGCAAGGTAGCTGTGTGGAC-3'	5'-AACAGGAGAACAGAGGCTGGT-3'
3	280 bp	5'-GAAACCTCCCAAAGAAGGAAG-3'	5'-GGAAGTGCCTCCACATGAA-3'
4	265 bp	5'-TAAAGCCTTCTGGAAGTCAGG-3'	5'-AACCCTCCCAAATGGATAA-3'
5	321 bp	5'-TGGGGTCCTTGGTAGACTTT-3'	5'-GGAAGTTCCCTCATTCACTCC-3'
6	222 bp	5'-ACATTGGTTGGTTCAACTTGC-3'	5'-GCTTTTGCCAAGCTATTCAGA-3'
7	234 bp	5'-GTGATGGTGCCATCCTTCTG-3'	5'-CCCTCTTAGGTACCCATCTCC-3'
8	363 bp	5'-TCTAGTACTCGCCGTGCACAT-3'	5'-GGAAACCAATTCAAACCTCCT-3'
9	220 bp	5'-TCAGTAAGGGTGTGTGTTTCTCA-3'	5'-CCCAAGTAAACCTCAGCACAG-3'
10	349 bp	5'-CCAGAGTGGTCACTGGGTAAT-3'	5'-TTCAACAGTGCTTCTCCGAAA-3'